

Transversal Kerr effect of $\text{In}_{1-x}\text{Mn}_x\text{As}$ layers prepared by ion implantation followed by pulsed laser annealing

Gan'Shina, E.; Golik, L.; Kun'Kova, Z.; Bykov, I.; Novikov, A.; Rukovishnikov, A.; Yuan, Y.;
Zykov, G.; Böttger, R.; Zhou, S.;

Originally published:

June 2016

Japanese Journal of Applied Physics 55(2016), 07MF02

DOI: <https://doi.org/10.7567/JJAP.55.07MF02>

Perma-Link to Publication Repository of HZDR:

<https://www.hzdr.de/publications/Publ-24004>

Release of the secondary publication
on the basis of the German Copyright Law § 38 Section 4.

Transversal Kerr effect of $\text{In}_{1-x}\text{Mn}_x\text{As}$ layers prepared by ion implantation followed by pulsed laser annealing

Elena Gan'shina^{1*}, Leonard Golik², Zoya Kun'kova², Igor Bykov³, Andrey Novikov¹, Alexander Rukovishnikov², Ye Yuan⁴, Georgy Zykov¹, Roman Böttger⁴, and Shengqiang Zhou⁴

¹ *Department of Physics, Moscow State University, Moscow 119991, Russia*

² *Institute of Radioengineering and Electronics, RAS, Fryazino 141190, Russia*

³ *Institute for Theoretical and Applied Electromagnetics, RAS, Moscow 125412, Russia*

⁴ *Helmholtz-Zentrum Dresden - Rossendorf, Institute of Ion Beam Physics and Materials Research, 01328 Dresden, Germany*

E-mail: eagan@mail.ru

$\text{In}_{1-x}\text{Mn}_x\text{As}$ ($x = 6.9\%$) layers prepared by ion implantation and subsequent pulsed laser annealing have been studied using the magneto-optical transversal Kerr effect (TKE) and spectral ellipsometry. Ellipsometry data reveal the good crystal quality of the layers. The samples show ferromagnetic behaviour below 77 K. Near the absorption edge of the parent InAs semiconductor, large TKE values are observed. In the energy regions of the transitions in the Γ and L critical points of the InAs Brillouin zone, there are several clearly defined structures in the low-temperature TKE spectra. We have calculated the spectral dependences of the diagonal and nondiagonal components of the permittivity tensor (PT), as well as the spectrum of magnetic circular dichroism (MCD) for our samples. A number of extrema in the obtained MCD and PT spectra are close to the energies of transitions in the critical points of the parent semiconductor band structure, which confirms the intrinsic ferromagnetism of the Mn-doped InAs layers.

1. Introduction

Diluted magnetic semiconductors (DMS), particularly (Ga,In)MnAs, attract much interest owing to their potential for spintronics and novel magneto-optical device functionalities. It is generally accepted that the holes donated by the substitutional Mn atoms mediate the ferromagnetic order of the localized Mn spins.¹⁻³⁾ Despite a considerable number of experimental and theoretical studies, the electronic structure of these materials, character of the holes, as well as mechanism of the ferromagnetic order in them are still not well understood. Magneto-optical (MO) spectroscopy is a powerful tool for probing the electronic structure of DMS systems. Magneto-optical Kerr effect (MOKE) spectra have to display the peculiarities associated with the intrinsic ferromagnetism (such as spin-split interband transitions between valence and conduction bands of the matrix) and the peculiarities associated with the presence of different magnetic inclusions (MnAs, Mn-atomic cluster, etc.), as well as with the spin-dependent transitions including the Mn impurity band. Most MO studies of In(Ga)MnAs have been performed using layers fabricated by low-temperature molecular beam epitaxy (LT-MBE).⁴⁻⁹⁾ At the same time, when alternative methods are used, other defects may arise in the growth process, which can have a significant impact on the character of impurity states, concentration of itinerant holes, and Fermi level location. Therefore, studies of In(Ga)MnAs grown by other techniques may provide additional information on the details of the electronic structure.

In our previous studies, we investigated the MO properties of In(Ga)MnAs layers prepared by laser ablation.¹⁰⁻¹²⁾ Usually, the Curie temperatures (T_C) of such samples were around room temperature. However, investigation of the MOKE spectra revealed that, at room temperature, their spectral peculiarities are related to the presence of ferromagnetic MnAs inclusions.

In this work, we utilized the magneto-optical transversal Kerr effect (TKE) and optical techniques to study the properties of $\text{In}_{1-x}\text{Mn}_x\text{As}$ ($x = 6.9\%$) layers prepared by ion implantation followed by pulsed laser annealing in order to reveal and separate the signals from different magnetic phases, as well as to explore the behaviour of spectral peculiarities conditioned by the ferromagnetism of the (In,Mn)As semiconducting matrix.

2. Experimental methods

Apart from LT-MBE, ion implantation is an alternative nonequilibrium method to introduce several orders more Mn into In(Ga)As than under solid equilibrium conditions.¹³⁻¹⁴⁾ Pulsed

laser annealing (PLA) on a time scale of nanoseconds is the only effective method of fabricating a metastable diluted magnetic semiconductor from Mn-implanted In(Ga)As or GaP.¹⁵⁾ During PLA, the near-surface region of the material melts, cools down within several microseconds, and solidifies epitaxially onto the host semiconductor. The fast cooling rate of PLA prevents diffusion and thus the formation of secondary phases. By optimizing the PLA parameters, it is expected that a large hole concentration can be realized in Mn-implanted In(Ga)As.

Unlike GaMnAs, few studies have been conducted on the MO properties in wide temperature and spectral ranges for the narrow-bandgap InMnAs semiconductor.^{4,5,8,16)} To the best of our knowledge, there are no investigations on the MO properties of InMnAs DMS prepared by Mn implantation with subsequent PLA until now.

The $\text{In}_{1-x}\text{Mn}_x\text{As}$ layers on InAs(001) substrates with $x = 6.9\%$ were prepared by ion implantation. Ion implantation was performed at room temperature at the Ion Beam Center at the Helmholtz-Zentrum Dresden-Rossendorf. Mn ions were implanted into intrinsic InAs(001) wafers at the energy of 100 keV at an incidence angle of 7° to avoid ion channeling. According to SRIM simulations, the Mn concentration was planned to be $x = 0.08$ considering a fluence of $1.6 \times 10^{16} \text{ cm}^{-2}$. A coherent XeCl excimer laser with 308 nm wavelength and 28 ns duration was used to anneal the implanted InAs layer. The profile of the laser beam was homogenized to $5 \times 5 \text{ mm}^2$. The annealing energy was optimized to be 0.2 J/cm^2 . However, the laser annealing made the amount of implanted Mn atoms (inside the InAs layer) diverge from the planned value, because part of the implanted Mn atoms diffused to the surface during the recrystallization procedure. Later on, the sample surface was etched in concentrated HCl to remove the inert surface layer. Nevertheless, most of the Mn atoms still remain inside the InAs matrix, and the final Mn concentration x was determined as 0.069 by particle-induced X-ray emission (PIXE). The effective thickness of the implanted layer was 80 nm. More details are shown in Ref. 17. Magnetometry was performed using MPMS 3 (SQUID-VSM) magnetometer from Quantum Design. Employing standard magnetometry measurements, we found that the $\text{In}_{1-x}\text{Mn}_x\text{As}$ layer is ferromagnetic at temperatures below 77 K.¹⁷⁾

The magneto-optical properties were studied in transversal geometry. The TKE consists of an intensity variation of the p-polarized light reflected by the sample under magnetization. The value $\delta = [I(H) - I(-H)]/2I(0)$, where $I(H)$ and $I(0)$ are the reflected light intensities in the presence and absence of a magnetic field, respectively, was directly measured in the experiment. An alternating magnetic field up to 240 kA/m was aligned

parallel to the sample surface and perpendicular to the light incidence plane. The sensitivity of the apparatus was $\approx 10^{-5}$.¹⁸⁾ The TKE spectra $[\delta(E)]$ were recorded in the energy range of $E = 0.5 - 4.0$ eV at different angles of light incidence defined from normal to the sample surface. The temperature range for the studies was $T = 15 - 300$ K. Temperature dependences $[\delta(T)]$ as well as TKE dependences on magnetic field $[\delta(H)]$, characterizing the magnetic state of the layers, were measured at some fixed energies. Spectra of the ellipsometry parameters, $\tan\psi(E)$ and $\cos\Delta(E)$, were recorded in the energy range of $E = 0.55 - 6.5$ eV at room temperature, using the ellipsometer SE 850 DUV (SENTECH Instruments).

3. Results and discussion

TKE spectra measured at different angles of light incidence at $T = 17$ K are shown in Fig. 1. As one can see, near the absorption edge of the semiconducting matrix ($E_g \approx 0.4$ eV), large TKE values ($\pm 6 \times 10^{-2}$) are observed, which are an order of magnitude larger than that for Mn-doped In(Ga)As ($\sim 7 \times 10^{-3}$) with different concentrations.¹⁰⁻¹²⁾ The spectral location of TKE band 1 is close to the $E_0 + \Delta_0$ transition energy (0.78 eV), and the positive band 2 that exceeds our measurement limit is apparently associated with the E_0 transition (0.4 eV) in the Γ critical point of the InAs Brillouin zone.¹⁹⁾ The significantly weaker structure 3, which also consists of positive and negative bands, is observed in the region of the E_1 , $E_1 + \Delta_1$ transitions (2.5 and 2.8 eV, respectively) near the L critical point of the InAs band structure (inset of Fig. 1). In addition, a feature in the region $E = 1.2 - 2.0$ eV (band 4) can be seen in the TKE spectra. The TKE spectra of Mn-doped InAs prepared by ion implantation significantly differ in shape from those of InMnAs samples prepared by laser ablation (Fig. 2). The TKE spectra of the latter are due to the presence of the ferromagnetic MnAs nanoclusters.¹²⁾

The temperature dependences $[\delta(T)]$ measured at two energies are presented in Figs. 3(a) and 3(b). The Curie temperature T_C , derived from the $\delta(T)$ dependence, which was obtained near the L point, coincides very well with the value determined from the magnetometry measurement, as shown in Fig. 3(c). At the same time, the $\delta(T)$ curve recorded for band 4 shows that this band appears at a temperature exceeding T_C . Further cooling leads to the change of the TKE sign at temperatures lower than T_C . One can conclude that in the region in band 4, we see the competition of the TKE contributions from transitions with different temperature dependences. Such behaviour of the $\delta(T)$ curve may indicate the presence of some second magnetic phase in a near-surface layer.

In Fig. 4(a), the dependence of the TKE value on magnetic field amplitude

measured for the $\text{In}_{0.931}\text{Mn}_{0.069}\text{As}$ layer at $T = 50$ K is shown. Figure 4(b) shows the directly measured field dependence of the magnetization at 50 K by SQUID-VSM magnetometry. Both curves exhibit a similar shape, indicating the ferromagnetic ordering of the sample. However, the saturation field values in the dependences obtained by the magneto-optical measurements are significantly larger, which could be related to both the large magnetic anisotropy of the near-surface layer and the presence of the second magnetic phase. Since this second magnetic phase is detected only by the magneto-optical measurements and it is indistinguishable in the magnetization measurements conducted for the sample as a whole, one can assume that the second magnetic phase is located in the near-surface layer and its volume is small, so the sample is mostly $\text{In}_{0.931}\text{Mn}_{0.069}\text{As}$.

We also performed ellipsometry measurements to determine the spectra of the real and imaginary parts, $\langle \varepsilon_1 \rangle$ and $\langle \varepsilon_2 \rangle$, respectively, of the diagonal components of the pseudodielectric function (Fig. 5). As seen in Fig. 5, peaks corresponding to the optical transitions near the L and X critical points of the Brillouin zone of InAs are present in the $\langle \varepsilon_2 \rangle(E)$ spectrum of our sample. Therefore, we can conclude that the crystal structure of the InAs parent semiconductor is conserved in the layer under study. An increase in matrix imperfection when the Mn dopant is introduced is a possible reason for decreasing the maxima and smearing the doublet ($E \approx 2.5 - 2.8$ eV), as well as for the increase in the $\langle \varepsilon_2 \rangle$ values in the region $E \approx 1.0 - 2.4$ eV. The transformation of the $\langle \varepsilon_1 \rangle(E)$ and $\langle \varepsilon_2 \rangle(E)$ dependences in the energy region $E < 2$ eV is also associated with the light interference in the layer under study.

The interference contribution appears and rises below the E_1 transition in the L-point, where the optical absorption in the semiconducting matrix abruptly decreases and the depth of the light penetration into the sample increases. The interference may be a reason for the downturn in the $\langle \varepsilon_1 \rangle(E)$ dependence in the range $E < 0.8$ eV, as well as of the minimum in the $\langle \varepsilon_2 \rangle(E)$ one near $E = 0.75$ eV.

We have used the $\langle \varepsilon_1 \rangle(E)$ and $\langle \varepsilon_2 \rangle(E)$ dependences together with the TKE spectra to calculate spectra of the real and imaginary parts of off-diagonal components, $\varepsilon' = \varepsilon'_1 - i\varepsilon'_2$ ($\varepsilon_{xy} = -i\varepsilon'$), of the permittivity tensor (PT). Following the formulas from Ref. 20:

$$\delta = a\varepsilon'_1 + b\varepsilon'_2,$$

$$a = 2 \sin 2\varphi \frac{A}{A^2 + B^2}, \quad b = 2 \sin 2\varphi \frac{B}{A^2 + B^2}, \quad (1)$$

$$A = \varepsilon_2(2\varepsilon_1 \cos^2 \varphi - 1), \quad B = (\varepsilon_2^2 - \varepsilon_1^2) \cos^2 \varphi + \varepsilon_1 - \sin^2 \varphi,$$

where the angle φ is the incidence angle, and using $\delta_1(\varphi_1, E)$ and $\delta_2(\varphi_2, E)$ values from the TKE spectra recorded at $T = 17$ K at two different angles of light incidence, $\varepsilon'_1(E)$ and $\varepsilon'_2(E)$ can be found. The calculated $\varepsilon'_1(E)$ and $\varepsilon'_2(E)$ dependences are presented in Fig. 6. The reported energies of the E_0 , $E_0 + \Delta_0$, and $E_1 + \Delta_1$ transitions in the Γ and L critical points of the Brillouin zone in InAs¹⁹⁾ are also shown in Fig. 6 by the vertical lines. One can see that a number of peculiarities are near the Γ and L critical points in the spectra of the off-diagonal PT components.

The obtained $\varepsilon'_1(E)$ and $\varepsilon'_2(E)$ spectra allowed us to calculate the spectral dependences for other magneto-optical effects and compare our data with the published MO spectra of (In,Mn)As. Magnetic circular dichroism (MCD) spectroscopy is the most common method of detecting and studying peculiarities in the electronic structure of (In,Ga)MnAs, since MCD spectra are the most simple to interpret.²¹⁾ Employing the $\varepsilon'_1(E)$ and $\varepsilon'_2(E)$ dependences together with the optical constants spectra, we calculated the transmission MCD spectrum for our $(\text{In}_{1-x}\text{Mn}_x)\text{As}$ sample.

This MCD spectrum corresponding to $T = 17$ K is presented in Fig. 7(a), where the dashed lines show the energies of the transitions in the Γ and L critical points in InAs. The reflection MCD spectrum of the LT-MBE $(\text{In}_{1-x}\text{Mn}_x)\text{As}$ sample ($x = 8\%$)⁵⁾ is shown in Fig. 7(b) for comparison. In the MCD spectra of both our sample and the LT-MBE-grown (In,Mn)As,^{4,5,14)} the dispersive structure (3) near the L point is present. There is also the negative peak (2) near the Γ point (the E_0 transition) in the spectrum of our sample, as well as in the spectra of samples prepared by MBE. The strong negative contribution from an additional band (4, $E_{\text{max}} \approx 1.6$ eV) is apparently the reason for the absence of band (1) corresponding to the $E_0 + \Delta_0$ transition in our MCD spectrum. The ascertainment of the band 4 nature requires further investigation.

The extremum locations in the MO spectra of the sample under study are close to the energies of the transitions in the critical points of the parent semiconductor band structure. This fact, as well as the character of the temperature and magnetic field dependences of TKE, $\delta(T)$ and $\delta(H)$, respectively, confirms the intrinsic ferromagnetism of the $(\text{In}_{0.931}\text{Mn}_{0.069})\text{As}$ layer prepared by ion implantation and laser annealing. The energy position and polarity of the MCD bands (2 and 3) are consistent with the picture of the InAs band structure split by the antiferromagnetic p-d exchange interaction. As shown in Figs.

7(a) and 7(b), the features near the Γ and L critical points are expressed more evidently in the MCD spectrum of our sample than in that of the LT-MBE sample.

4. Conclusions

For the first time, the optical and magneto-optical properties of the Mn-doped InAs layer prepared by ion implantation with further laser annealing have been studied. Near the absorption edge, large values of TKE have been observed. The spectral dependences of the diagonal and nondiagonal components of the pseudodielectric tensor (PT) have been determined. The intrinsic ferromagnetism of the Mn-doped InAs layer is confirmed by the extrema positions in the MO and PT spectra close to the energies of the transitions in the critical points of the parent semiconductor band structure. The obtained results show that by ion implantation and laser annealing, it is possible to obtain (In,Mn)As/InAs DMS with ferromagnetic ordering, high magnetization, giant MO response, and high spin polarization.

Acknowledgments

This work was supported by the Russian Foundation for Basic Research N15-02-02077 and by the German Research Foundation (DFG, ZH 225/6-1). The ion implantation was performed at the Ion Beam Center at the Helmholtz-Zentrum Dresden Rossendorf. The work was supported in part by M.V.Lomonosov Moscow State University Program of Development.

References

- 1) T. Dietl and H. Ohno, *Rev. Mod. Phys.* **86**, 187 (2014).
- 2) T. Jungwirth, J. Wunderlich, V. Novák, K. Olejník, B. L. Gallagher, R. P. Campion, K. W. Edmonds, A. W. Rushforth, A. J. Ferguson, and P. Němec, *Rev. Mod. Phys.* **86**, 855 (2014).
- 3) M. Tanaka, S. Ohya, and P. Nam Hai, *Appl. Phys. Rev.* **1**, 011102 (2014).
- 4) K. Ando and H. Munekata, *J. Magn. Magn. Mater.* **272**, 2004 (2004).
- 5) A. Winter, H. Pascher, M. Hofmayer, H. Krenn, T. Wojtowicz, X. Liu, and J. K. Furduna, *Rev. Adv. Mater. Sci.* **20**, 92 (2009).
- 6) K. Ando, H. Saito, K. C. Agarwal, M. C. Debnath, and V. Zayets, *Phys. Rev. Lett.* **100**, 067204 (2008).
- 7) C. Sun, J. Kono, Y.-H. Cho, A. K. Wojcik, A. Belyanin and H. Munekata, *Phys. Rev. B* **83**, 125206 (2011).
- 8) P. Fumagalli and H. Munekata, *Phys. Rev. B* **53**, 15045 (1996).
- 9) P. Fumagalli, H. Munekata, and R. J. Gambino, *IEEE Trans. Magn.* **29**, 3411 (1993).
- 10) E. A. Gan'shina, L. L. Golik, V. I. Kovalev, Z. E. Kun'kova, B. N. Zvonkov, and A. N. Vinogradov, *J. Magn. Magn. Mater.* **321**, 829 (2009).
- 11) E. A. Gan'shina, L. L. Golik, V. I. Kovalev, et al *Solid State Phenom.* **168-169**, 35 (2011).
- 12) E. A. Gan'shina, L. L. Golik, V. I. Kovalev, Z. E. Kun'kova, A. G. Temiryazev, Yu. A. Danilov, O. V. Vikhrova, B. N. Zvonkov, A. D. Rubacheva, P. N. Tcherbak, A. N. Vinogradov, and O. M. Zhigalina, *J. Phys.: Condens. Matter* **22**, 396002 (2010).
- 13) M. A. Scarpulla, O. D. Dubon, O. Montiero, M. R. Pillai, M. J. Aziz, and M. C. Ridgway, *Appl. Phys. Lett.* **82**, 1251 (2003).
- 14) M. A. Scarpulla, B. L. Cardozo, R. Farshchi, W. M. Hlaing, M. D. McCluskey, K. M. Yu, and O. D. Dubon, *Phys. Rev. Lett.* **95**, 207204 (2005).
- 15) S. Zhou *J. Phys. D.* **48**, 263001 (2015).
- 16) P. T. Chiu and B. W. Wessels, *Appl. Phys. Lett.* **89**, 102505 (2006).
- 17) Y. Yuan, Y. Wang, K. Gao, M. Khalid, C. Wu, W. Zhang, F. Munnik, E. Weschke, C. Baetz, W. Skorupa, M. Helm, and S. Zhou, *J. Phys. D.* **48**, 235002 (2015).
- 18) E. A. Balykina, E. A. Gan'shina, and G. S. Krinchik, *Sov. Phys. JETP* **66**, 1073 (1987).
- 19) E. D. Palik and R. T. Holm, in *Indium Arsenide Handbook of Optical Constants of Solids*, ed. E. D. Palik (Academic Press, Orlando, 1985) p. 483.
- 20) G. S. Krinchik, *Physics of Magnetic Phenomena* (MSU Publications, Moscow, 1985) p. 294.

- 21) K. Ando, in *Magneto-Optics* (Springer, Berlin, 2000) ed. S. Sugano and N. Kojima (Springer Series in Solid State Science). Vol. 128, p. 211.

Figure Captions

Fig. 1. (Color online) TKE spectra of $\text{In}_{1-x}\text{Mn}_x\text{As}$ layer ($x = 6.9\%$) at $T=17$ K and different angles of light incidence. The numbers 1 – 4 denote different TKE bands described in the text. Inset: TKE spectrum near the L critical point of the Brillouin zone of InAs.

Fig. 2. (Color online) TKE spectra of InMnAs layer (sample 2) prepared by laser ablation¹²⁾ at $T = 293$ and 30K (solid and open symbols, respectively). Inset: Temperature dependence of TKE value at $E=1.06$ eV.

Fig. 3. (Color online) TKE value versus temperature measured in the regions of band 3 (a) and band 4 (b). (c) Temperature dependence of the remanent magnetization for the same $\text{In}_{1-x}\text{Mn}_x\text{As}$ ($x=6.9\%$) layer.

Fig. 4. (Color online) (a) Dependence of the TKE value on the magnetic field amplitude for the $\text{In}_{0.931}\text{Mn}_{0.069}\text{As}$ layer at $T = 50$ K and $E = 1.97$ eV. (b) Field dependence of magnetization at 50 K, measured by SQUID-VSM magnetometry, $H \parallel [110]$.

Fig. 5. (Color online) Spectral dependences of the real and imaginary parts of the pseudo-dielectric function, $\langle \varepsilon_1 \rangle(E)$ and $\langle \varepsilon_2 \rangle(E)$, respectively, for the $\text{In}_{0.931}\text{Mn}_{0.069}\text{As}$ sample at $T = 300$ K. Spectra $\varepsilon_1(E)$ and $\varepsilon_2(E)$ computed for an InAs layer using the tabulated data¹⁹⁾ are shown for comparison.

Fig. 6. (Color online) Spectral dependences of the real $\varepsilon'_1(E)$ (a) and imaginary $\varepsilon''_2(E)$ (b) parts of the off-diagonal components of PT for $\text{In}_{0.931}\text{Mn}_{0.069}\text{As}$. The energies of the E_0 , $E_0 + \Delta_0$, and E_1 , $E_1 + \Delta_1$ transitions in InAs are shown by vertical dashed lines.

Fig. 7. (Color online) MCD spectrum calculated for the (In,Mn)As layer under study (a) and the measured one for (In,Mn)As sample prepared by LT-MBE method (b).⁵⁾ Reprinted with permission from Copyright 2009 Advanced Study Center Co. Ltd. Ref.5.

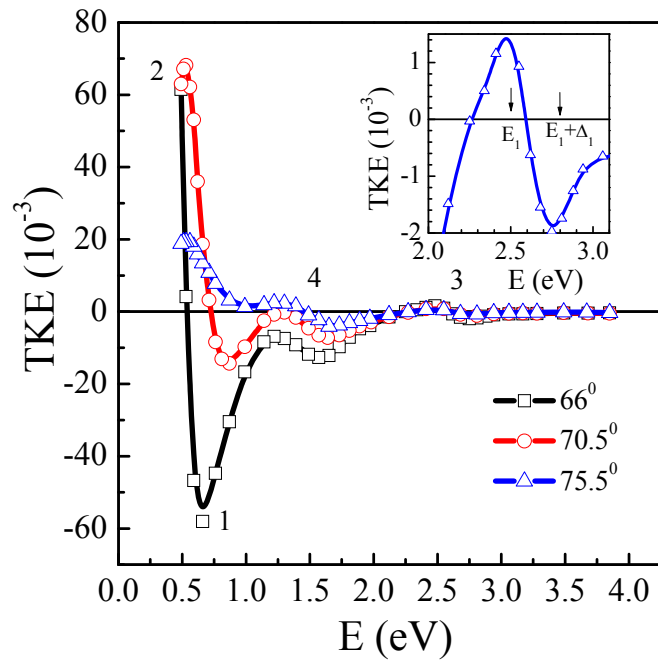


Fig.1

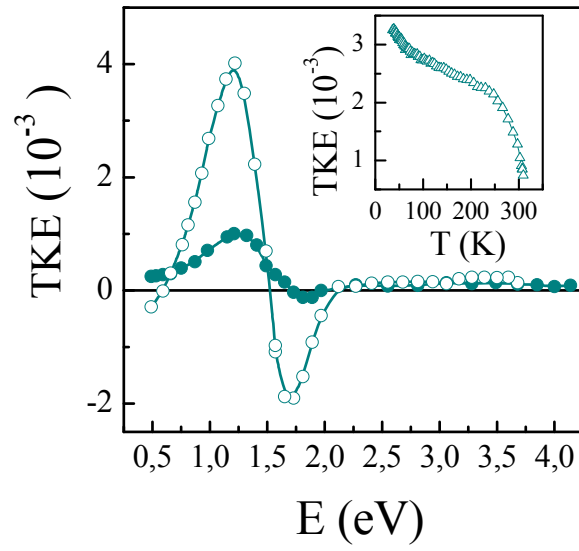


Fig.2

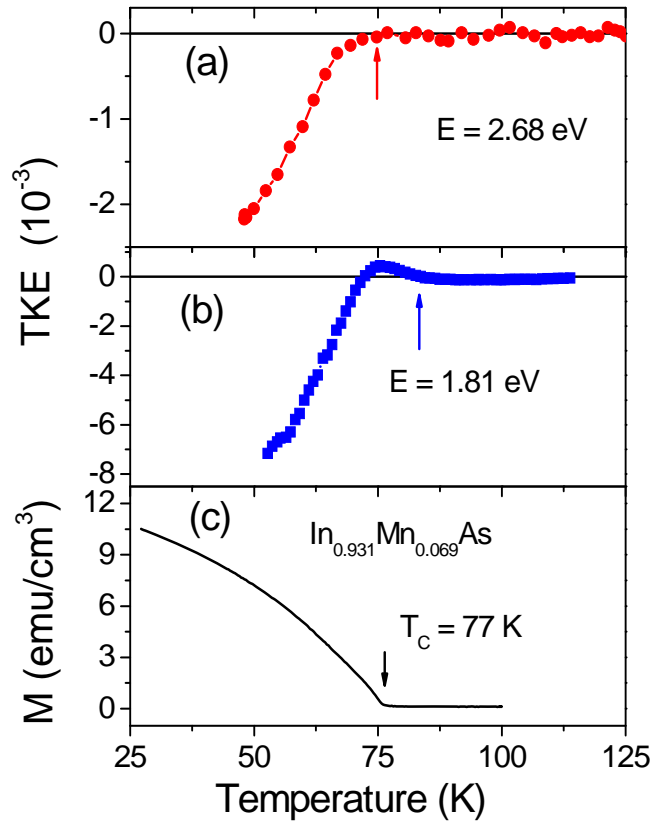


Fig.3

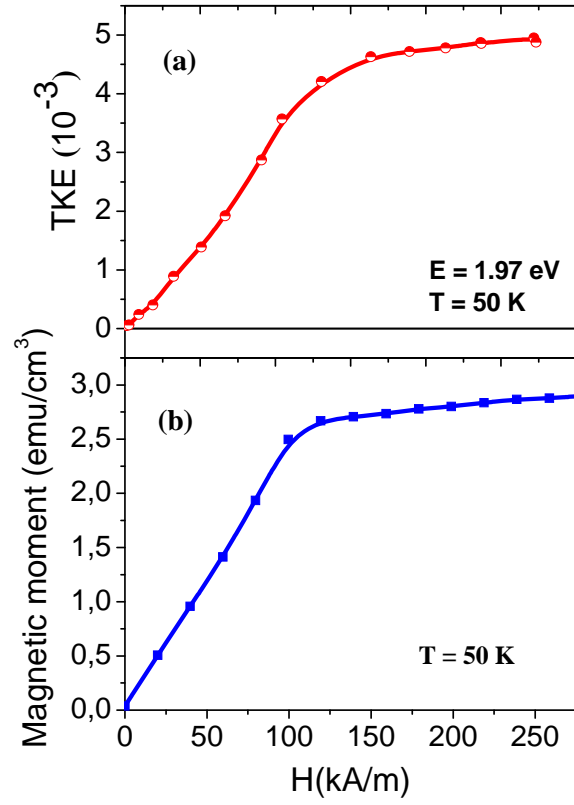


Fig.4

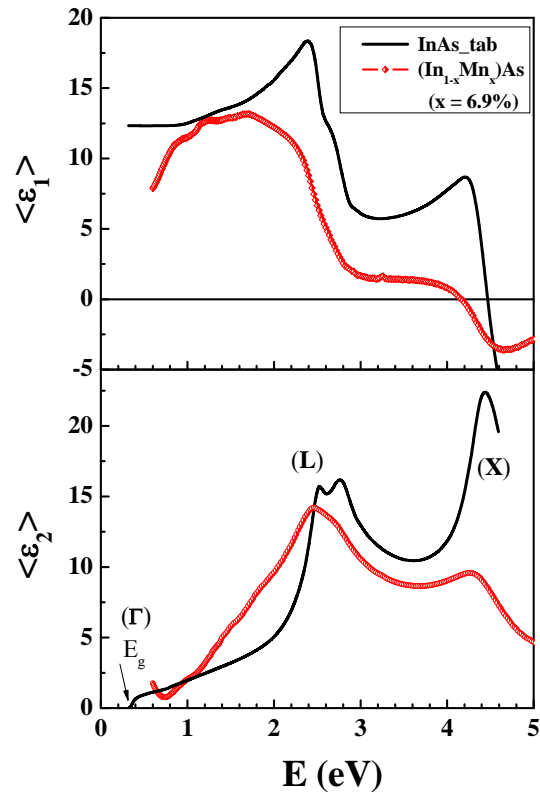


Fig.5

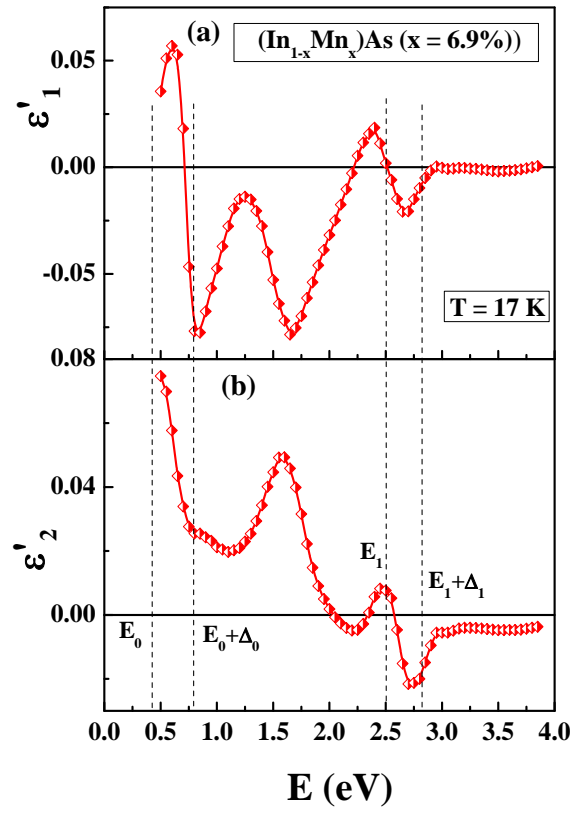


Fig.6

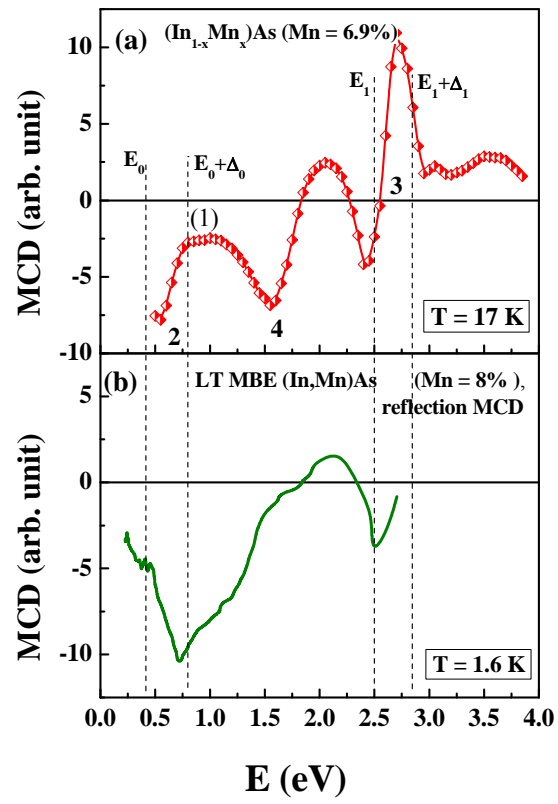


Fig.7